International Baccalaureate:

Extended Essay

Investigation of the Effect of Frequency of Light on the Efficiency of Solar Cells

Research Question: How does the Frequency of Photons, and thus Energy, Absorbed by the Solar Cell Influence the Power Output of the Cell?

Candidate Number: gyz777

May 2019

Subject: Physics

Referencing Type: Harvard

Word Count: 3995

Table of Contents

Introduction

1.1 Scope of Work

A key limitation of solar energy is the low efficiency conversion of a photon's energy into electrical energy, which is heavily influenced by temperature. Energy of a photon is proportional to its frequency so by changing the frequency of the light source, we can change the energy of the photons absorbed by the photovoltaic cell and monitor its efficiency. This investigation aims to obtain the optimum frequency and thus energy of the photon to maximise the efficiency of a solar cell by minimising temperature loss. This leads to the research question: **How does the Frequency of Photons, and thus Energy, Absorbed by the Solar Cell Influence the Power Output of the Cell?**

1.2 The Photoelectric Effect

Solar cells are based on the concept of the photoelectric effect which is defined as "the ejection of electrons from the surface of a metal in response to incident light" (Warren Davis, n.d.), providing the photon has enough energy to excite the electrons from its valance band to the conduction band. The energy of a photon is determined by the equation: $E = hf$, therefore frequency is proportional to energy.

The band gap is the gap between different states of excitation of an electron. Semi-conductors have a small enough band gap to gain energy levels by photons from visible light but not enough to be constantly excited and therefore are always in a free state. An electron only becomes excited and free to move when the energy of the photons absorbed by the silicon is sufficient to raise the electron state from the valence to the conduction band (Penn State University Department of Energy and Mineral Engineering, 2018). If the energy of the photon is greater than the band gap of the electron in the semi-conductor it will emit the electron. The excess photon energy will dissipate as kinetic energy of the photoelectron

and thus heat, increasing resistance and decreasing efficiency. **Therefore the optimum frequency and thus energy, is the exact same energy as the band gap – enough to dislodge the electron but no excess energy which would result in an unwanted increase of temperature.**

1.3 Shockley Queisser Limit

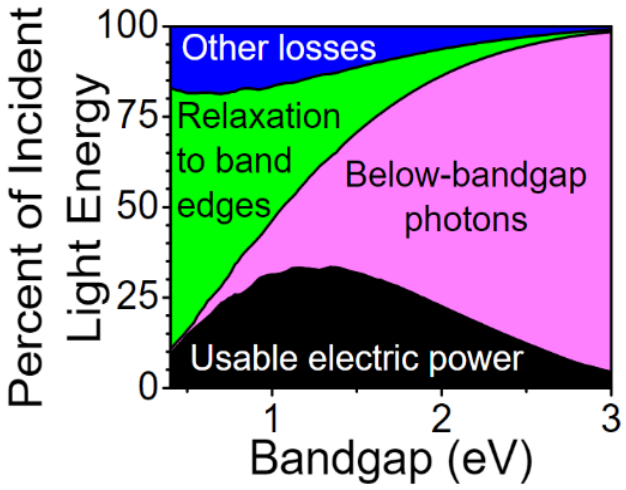

Figure 1: The Variation of band gap and light energy (Shockley Queisser , n.d.)

This graph demonstrates the Shockley-Queisser limit which is due to the following energy losses: photons being below than the bandgap (19% at 1.1 eV); relaxation to conduction band edges through electron relaxation (33% at 1.1 eV); other losses includes radiative recombination to maintain thermal equilibrium and energy loss due to the voltage less than the energy band.

Shockley and Queisser stated that there is a maximum of 33.7% efficiency of single junction cells due to the compromise between an increase in electrons becoming excited from a decrease in band gap, and the increase of excess energy resulting in thermalisation. Thermalisation is the “absorption of a high-energy photon [which] generates one electron-hole pair just as the absorption of a low-energy photon does. The extra energy of photons above the bandgap is lost via relaxation to low frequency phonons [thermal vibrations] and heat.” (Optoelectronics, Singlet Fission, 2015). This shows that frequency determines the power losses from relaxation, thermalisation and insufficient energy to raise electrons to the conduction band.

1.4 Singlet Fission

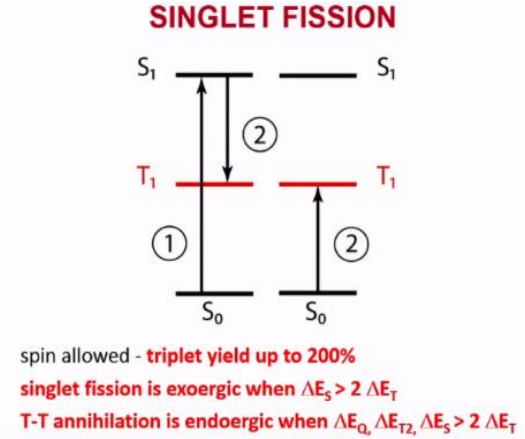

Figure 2: Singlet Fission energy diagram (Michl, n.d.)

This shows how one electron is being excited and the excess energy is released to a neighbouring electron, exciting two atoms. This can only occur depending on the precise energy and thus frequency of the photon.

Singlet fission is where excited electrons with higher energy levels than the band gap reduce in energy level, whilst still remaining excited, and fission to take place and release the excess energy to a neighbouring atom's electron and exciting that one, creating two pairs of electron gaps and thus doubling efficiency.

An increase in temperature in semi-conductors causes greater conductivity and fewer phonons which collide with the excited electrons, causing the electron to lose energy and reduce voltage. However, despite the decrease in thermal vibrations, the power output decreases with temperature. Heat causes electrons to be excited, raising the energy of the electron at rest. As the photovoltaic effect relies on generating power from the difference between rest state and excited state, the difference between the energy bands is smaller, causing less power at higher temperatures. **Therefore at higher frequencies there will be higher temperatures and thus lower power output** demonstrated below:

1.5 Recombination and Thermalisation

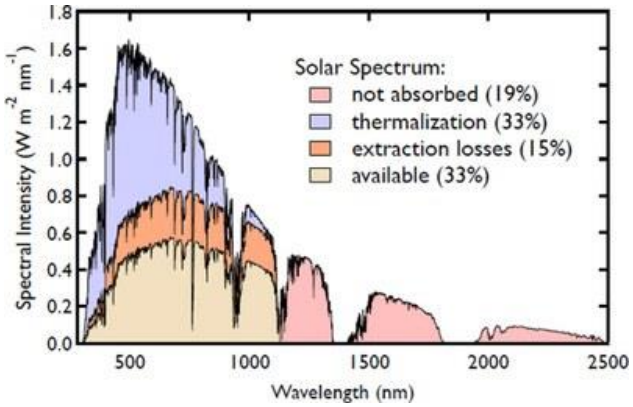

Figure 3: The variation of wavelength and Light intensity (Optoelectronics, Singlet Fission, 2015)

Similar to Figure 1, Figure 3 shows that shorter wavelengths, and therefore higher energy photons, result in increased inefficiencies, due to energy losses through thermalisation of light generated carriers

(S Riekeberg, 2006) found three inefficiencies causing higher than ambient temperature of solar cells: thermalisation of light generated carriers, recombination and resistive losses. Furthermore, (Radziemska, 2003) investigated how temperature affected the efficiency of solar cells and found a drop of output power of (−0.65%/K). This suggests that increasing frequency and thus energy over the band gap threshold, results in thermalisation which decreases power output of the cell.

Excess recombination is “when an electron which exists in the conduction band eventually stabilises to the lower energy valence band and moves into an empty hole on the valent band and removes a hole.” (Bowden, n.d.). In a steady state, the solar cell should have equal amounts of generation (where an electron moves from valent to conduction bands, leaving a hole) and recombination to maintain concentrations of electrons and holes in both the valence and conduction band. There are 3 types of recombination: Radiative, releasing energy as a photons; Shockley-Read-Hall, releasing energy as a photon or multiple phonons and Auger recombination where an electron is pushed high into the conduction

band and gradually thermalises as it relaxes. In the last two types, this can lead to increased thermalisation and decrease in efficiency.

Figure 4 shows the inefficiencies of recombination of light generated carriers, from the P-V junction, which is conditioned by the different frequencies of light which have different recombination collection properties. Blue light has more surface recombination and a high absorption coefficient and is unlikely to emit minority carriers, like phonons, therefore less thermalisation occurs. In contrary, red light has more bulk and rear surface recombination, which will generate carriers deep in the cell and are unlikely to collect in the junction generating heat.

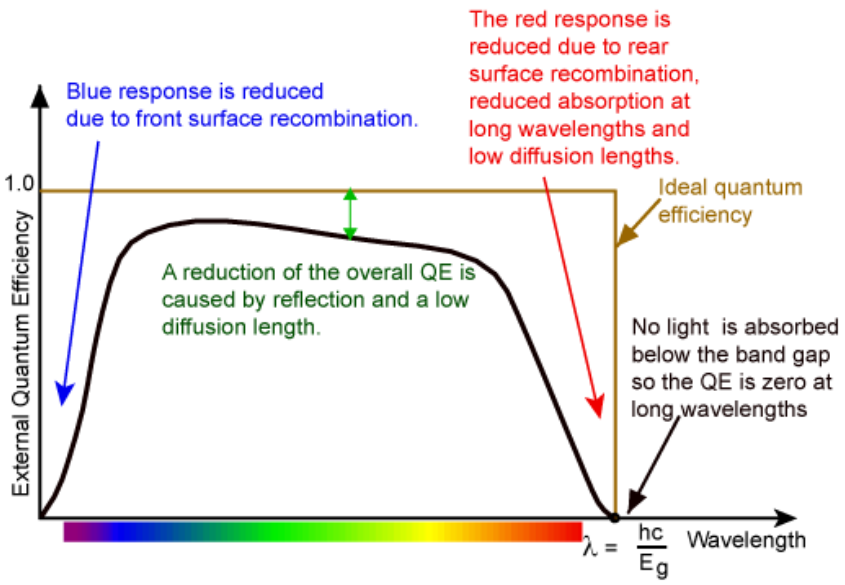

Figure 4: The current losses due to recombination (Current Losses Due to Recombination, n.d.)

1.6 Tilt Angle

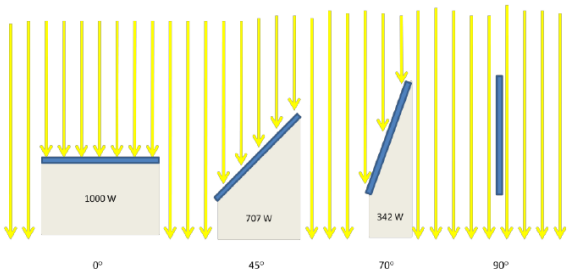

Figure 5: How increasing tilt angle limits the amount of solar irradiance reaching the solar panel (Challenges for Building Integrated Photovoltaics in the Agder Region, n.d.)

The tilt angle is an important factor in the efficiency of the solar panel and in addition to investigating how frequency of the photons affects the power output I will look at the tilt angle of the solar panel in relation to the light source.

Theoretically, the smaller the angle, the greater the solar irradiance and thus the greater the number of photons absorbed by the solar cell resulting in a greater power output as shown in figure 5. Furthermore, due to total internal reflection, increasing the tilt angle will increase the number of photons which are reflected instead of being refracted into the solar panel.

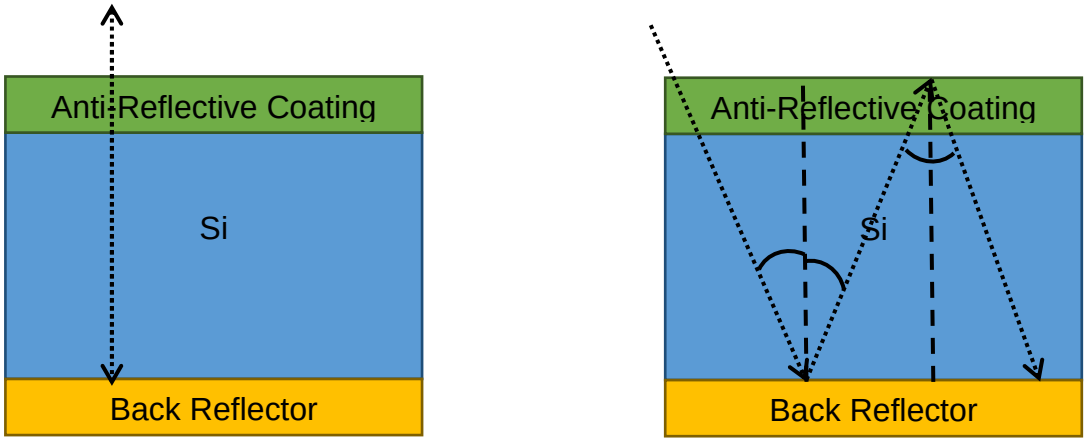

Figure 6: Diagram to show how photon at an angle travels a greater distance and is therefore more likely to be absorbed.

However, modern solar panels contain back reflectors at the bottom layer, causing photons which haven't been absorbed to be reflected back into the silicon. Therefore, an increased angle results in a greater distance for the photon to travel, increasing the probability of absorption. Total internal reflection can also occur if the light ray is greater than the critical angle further increasing the effect.

Experiment Set-up Design

N.B. The solar panel I used is a polycrystalline silicon PV cell with p-type gallium and n-type phosphorus and has a bandgap of 1.11eV.

2.1 Analysing filters to determine which wavelengths are passed through

To test how different frequencies of light impacted the power output, I used 9 filters which only allowed certain wavelengths of light through, to target 9 specific wavelengths of light from the visible light spectrum. I used this range as the filters have a variety of wavelengths and are well dispersed on the visible light spectrum.

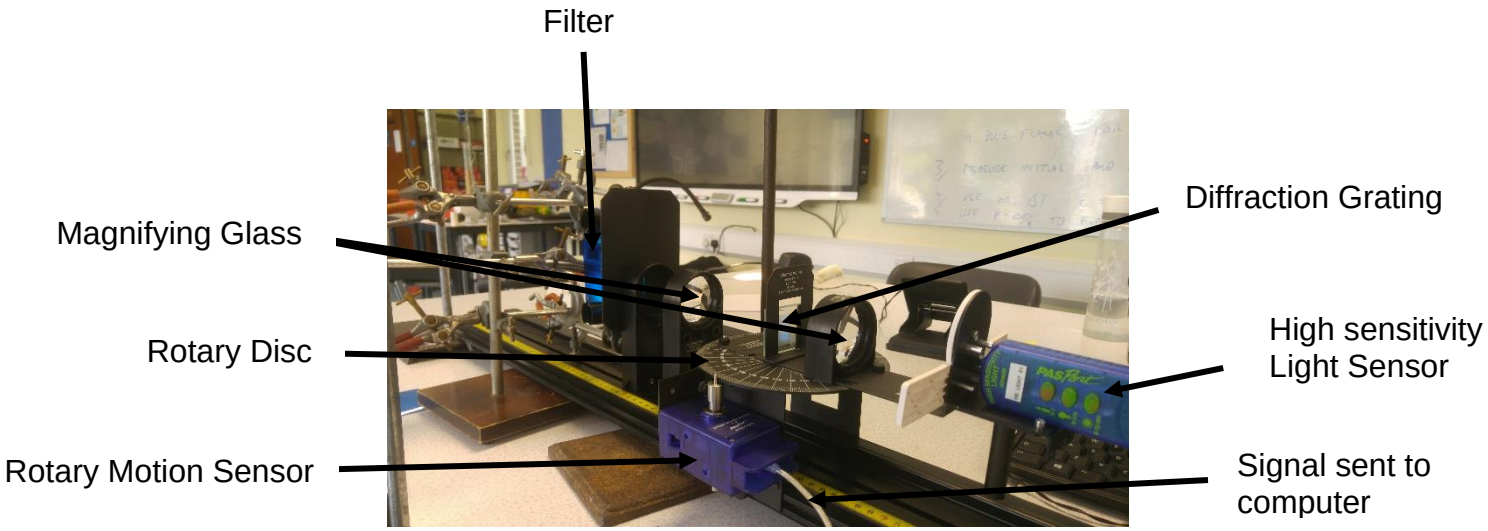

Figure 7: General setup of the Spectrophotometer

To calculate which wavelengths of light were able to pass through the filters, I used a spectrophotometer (PASPORT Educational Spectrophotometer, n.d.) and a 600 lines/mm diffraction grating.

I used the highest light intensity value (the local maximum on the graph) to calculate the wavelength of light which was let through by each filter, using the equation $n\lambda = d\sin(\theta)$.

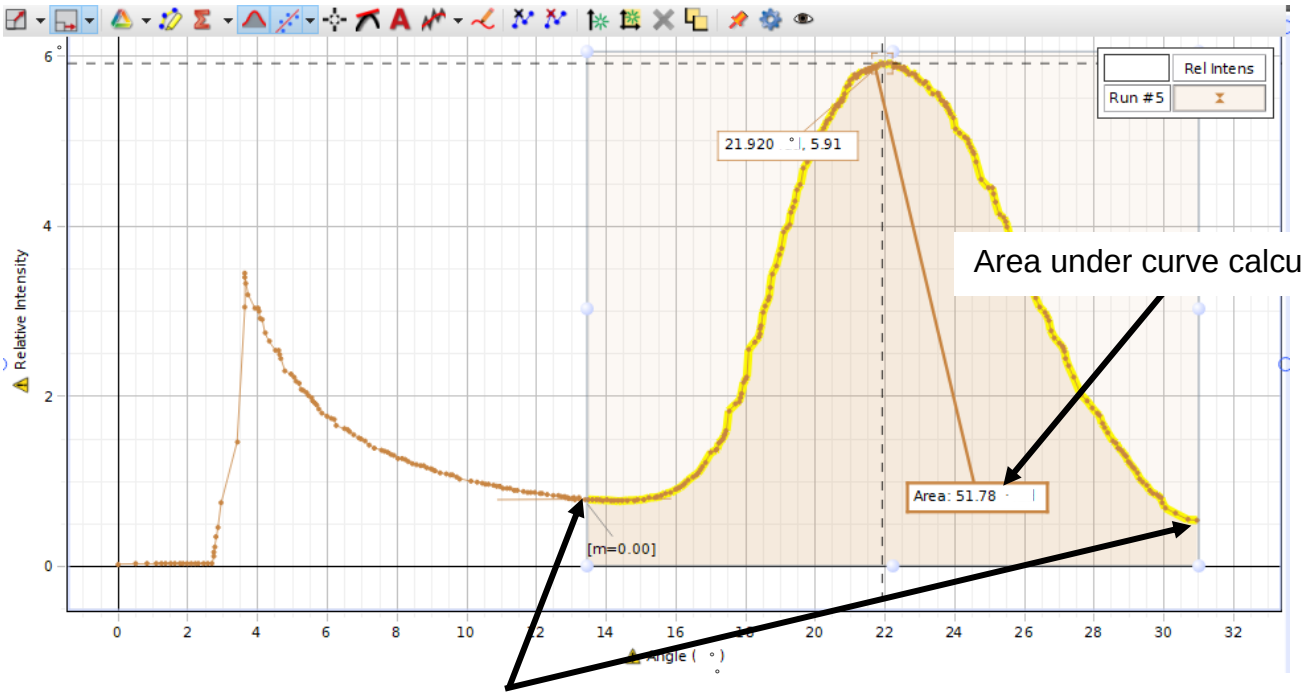

Figure 8: Pasco Capstone Area of Maximum calculation from "

As seen in figure 8, the minimum on the graph is not zero. This is due to the dark cloth which still allowed some light through and because of the sensitivity of the light sensor influenced the result.

Due to the inaccuracies mentioned above, I compared the data from figure 8 with the datasheet of the same filter, "Deep amber":

Filter	1	2	Mean/Deg	Mean/Rad	Wavelength/m	Wavelength/nm
Deep Amber	21.928	21.920	21.924	0.383	6.223E-07	622.294

Figure 9: Primary Data calculated using Pasco Software to determine maximum

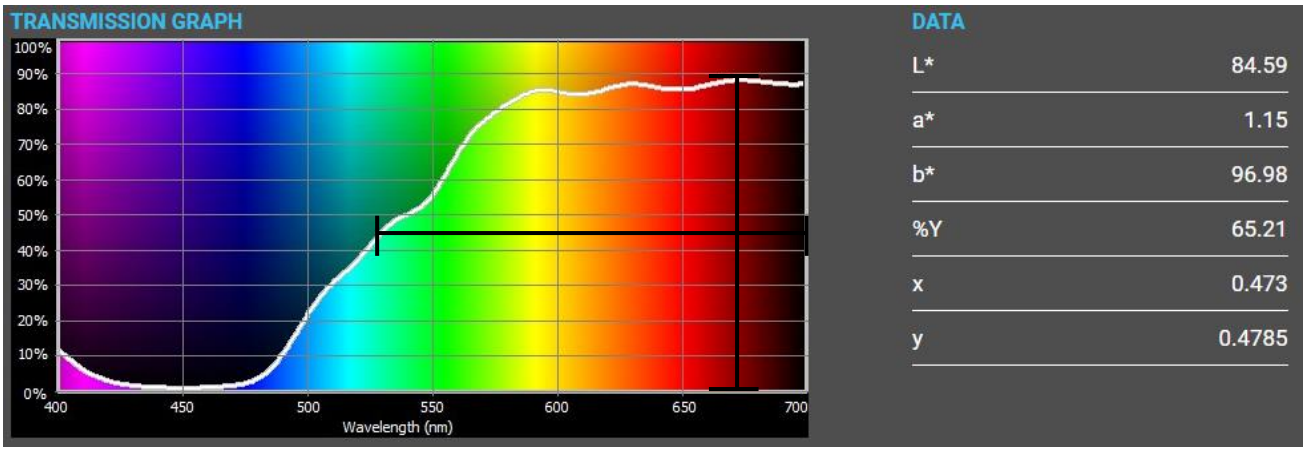

Figure 10: Secondary Data from datasheet (see appendix 1 for complete filter graphs)

When comparing the local maxima from both graphs, we get 622 nm for primary data and 670 nm from the datasheet. It is clear that there is a significant difference between both maxima. Presuming the results from the datasheet were obtained through greater precision and accuracy than the primary data, to aid the reliability of the investigation, **the data collected from the diffraction grating should be rejected and the datasheet values should be accepted.**

All the filters allowed a range of wavelengths through, some let in a greater range than others, resulting in a higher intensity of light leaving the filter. I changed from power output to a corrected power output: **power output / percentage of light transmission** through filter (% Y on datasheets).

To show that intensity is proportional to power output, I conducted another experiment: the effect of distance from solar cell against power output. From the inverse square relationship, as distance is doubled light intensity should decrease by a factor of two.

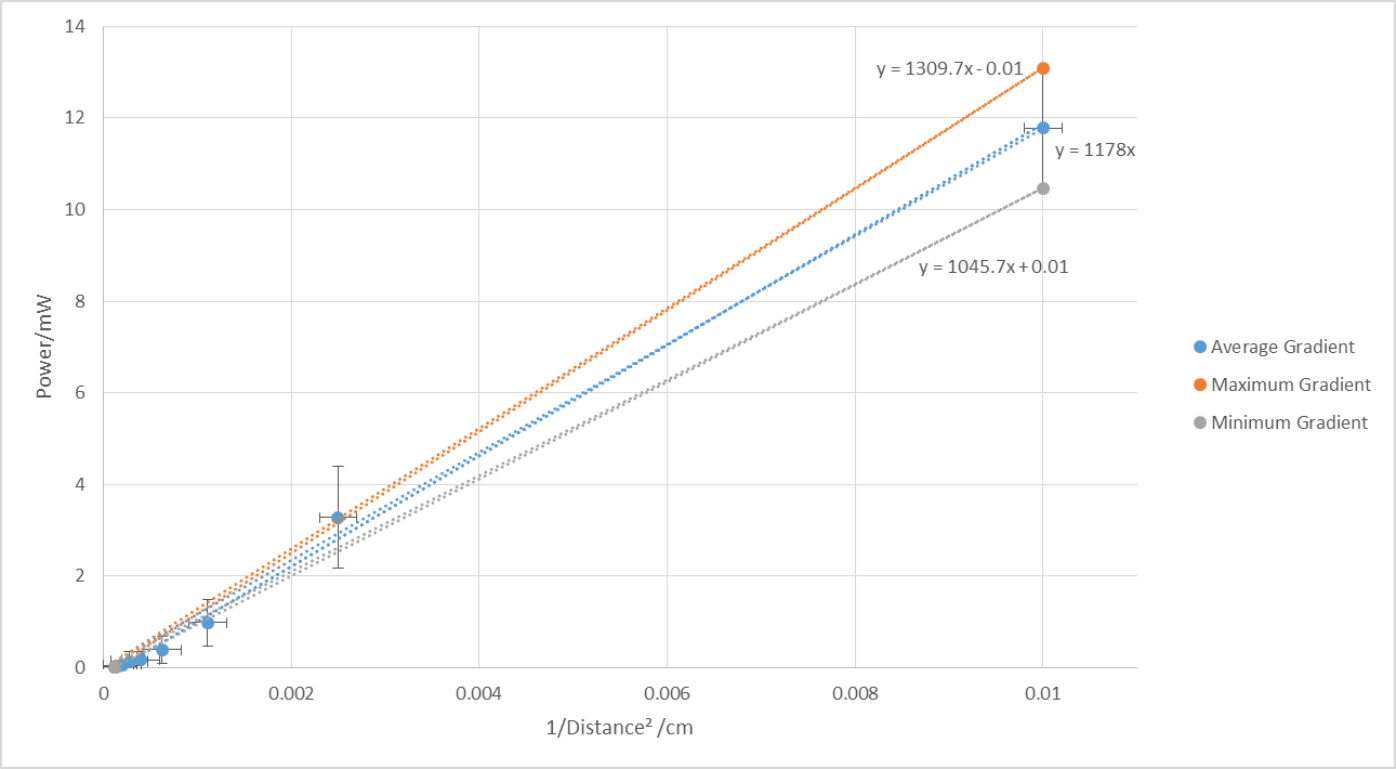

Figure 11: Graph of how the power output at different distance from the light source affects the inverse power output squared

I plotted 1/distance² against power output to show that the trend line intersects the origin. As seen by the equation of the line it does intersect at (0,0) and the minimum and maximum gradient shows the intersect to be ±0.01 mW. This uncertainty is low enough to show that **intensity is proportional to power output and validates experiment 1.**

Cutting the light intensity by using a filter, I can expect that power output is proportional to light intensity and if it is not proportional, then it is likely to be the frequency of the photons which is causing the change.

2.2 Measuring the Power Output of the Solar Cell

I chose power as the best way to measure the relative efficiency of the solar cell, as voltage and current change independently due to conductivity, resistance and difference in band gaps. Power is also a universal method in terms of output and determining the maximum power output that the cell can generate under ideal conditions is a sufficient test of efficiency.

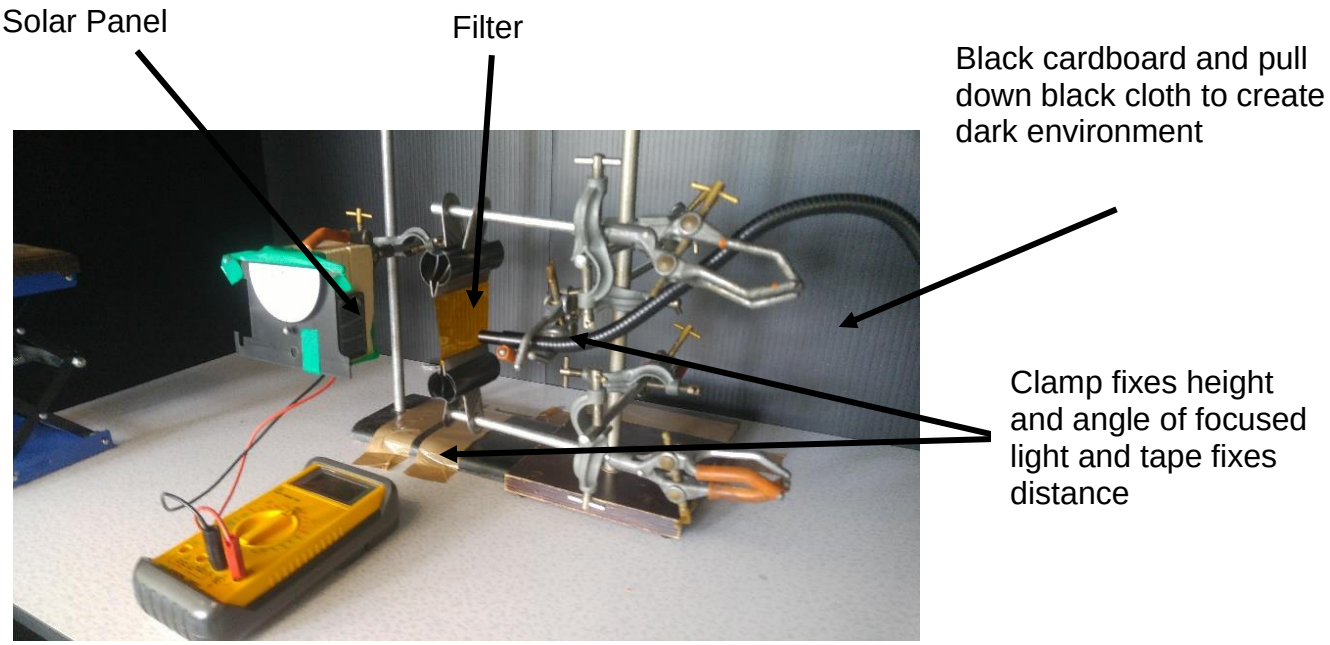

Figure 12: General setup of measuring the power output using different filters

To control the variables of height, angle and distance of the light source, I fixed the light source. I darkened the area so as little light could enter as possible and prevent variations in environment light from altering the efficiency of the solar panel.

One of the main disadvantages to this method is the rapid decrease in power output, most likely from the heat of the lamp, reducing efficiency. To make this a fair test, I measured both the voltage and current at its highest values, before the heat decreased efficiency. I also repeated the procedure 5 times replacing the filter every recording to ensure I did not have one group of filters which took place at the end where temperature inevitably was at the highest.

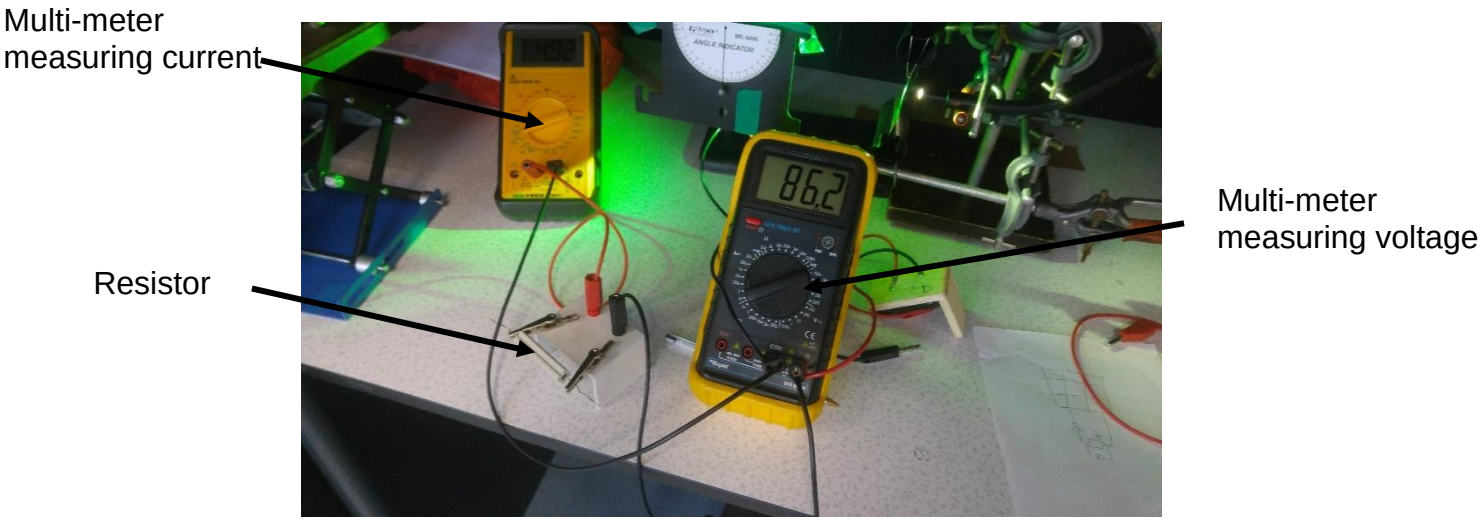

Figure 13: Measuring the power output from current and voltage readings

I placed a resistor, to act as a load and measured in parallel. To calculate power I used the equation P=IV before dividing by light transmission through filter (obtained from filter datasheet).

2.3 Measuring tilt angle of solar cell against power output

Figure 14: Inclinometer attached to solar panel mount

In addition to the main experiment I will be looking at how tilt angle of the solar panel, in relation to the light source, affects the power output. By rotating the clamp, I was able to get an uncertainty of ±0.5° using the analogue angle indicator.

Results from Recorded Data

3.1 Power Output using Different Filters

Deep Straw	Trial 1	Trial 2	Trial 3	Trial 4	Trial 5	Mean	σ	$\sigma\bar{x}$
Current/mA	9.30	8.02	8.50	8.56	8.22	8.52	0.49	0.22
Voltage/mV	162.3	141.6	148.8	148.4	143.7	149.0	8.06	3.61
Power/mW	1.51	1.14	1.26	1.27	1.18	1.27	0.13	0.06

Figure 15: Example of Raw and Processed Data of Power Output using "Deep Straw" filter

See Appendix 2 for raw data. Uncertainty for current and voltage is noted above derived from the multi-meter accuracy where current could only be measured to two decimal places, and voltage to one decimal place. Standard Deviation (σ) was calculated by Excel and I used the 68–95–99.7 rule to identify any anomalies.

3.2 Uncertainty for wavelengths transmitted through filter

Due to the range of light that passes through the filter, the maximum or dominant wavelength cannot be determined as the direct cause for the corrected power output efficiency. Therefore, the error bars were calculated by halving the maximum intensity and reading the range of nm at that height (see figure 10 for method).

Name of Filter	Dominant Wavelength/nm	Frequency of Photon/THz	Energy of Photon/eV
Deep Straw	598	501.33	2.07
Primary Red	624	480.44	1.99
Deep Amber	578	518.67	2.15
Orange	591	507.26	2.10
Lagoon Blue	481	623.27	2.58
Dark Green	515	582.12	2.41
Medium Blue	473	633.81	2.62
Light Blue	479	625.87	2.59
Fern Green	538	557.24	2.30

Figure 16: Conversion of Wavelength to Frequency and Energy of Photon

To find the frequency I used the equation $V=f\lambda$, where V was speed of light in a vacuum. I used $e=hf$, where h is Planck's constant, to find energy of the average photon passing through the filter. I converted it into Tera Hertz which was easier to interpret, similarly with energy where I converted from joules to eV by multiplying by 6.242×10^{18}.

3.3 Power Output with variation of Tilt Angle of Solar Panel

	Angle/° (±0.5°)	0	5	10	15	20	25	30	35	40	45	50	55	60
Power/mW	Trial 1	1.97	2.09	2.34	2.38	2.38	2.34	2.21	2.10	1.76	1.17	0.45	0.08	0.01
	Trial 2	1.89	2.05	2.26	2.30	2.38	2.44	2.30	2.02	1.60	1.06	0.50	0.08	0.02
	Trial 3	1.99	2.07	2.22	2.41	2.43	2.44	2.36	2.15	1.79	1.25	0.56	0.06	0.01
	Trial 4	1.96	2.16	2.31	2.43	2.46	2.39	2.24	1.98	1.53	0.84	0.22	0.03	0.01
	Trial 5	1.98	2.06	2.25	2.41	2.48	2.43	2.35	2.11	1.80	1.29	0.59	0.13	0.01
	Mean	1.96	2.09	2.28	2.39	2.43	2.42	2.31	2.11	1.75	1.21	0.53	0.09	0.01
	Standard Deviation	0.04	0.04	0.05	0.05	0.05	0.04	0.06	0.07	0.12	0.18	0.14	0.04	0.00
	Standard Error	0.018	0.019	0.022	0.022	0.020	0.020	0.029	0.032	0.055	0.079	0.065	0.016	0.002

Figure 20: Processed Data of how tilt angle affects Power Output of Solar Panel

See Appendix 4 for raw data. The tilt of the solar panel was measured to the nearest degree, hence ±0.5°. Standard deviation and standard error was calculated using the same method as 3.1 data and standard error was used as the vertical error bars for power uncertainty.

Graphs showing how Power Output is affected by Different Factors

4.1 Graph 1 and Analysis of how the mean frequency of a photon affects the power output per percent transmission

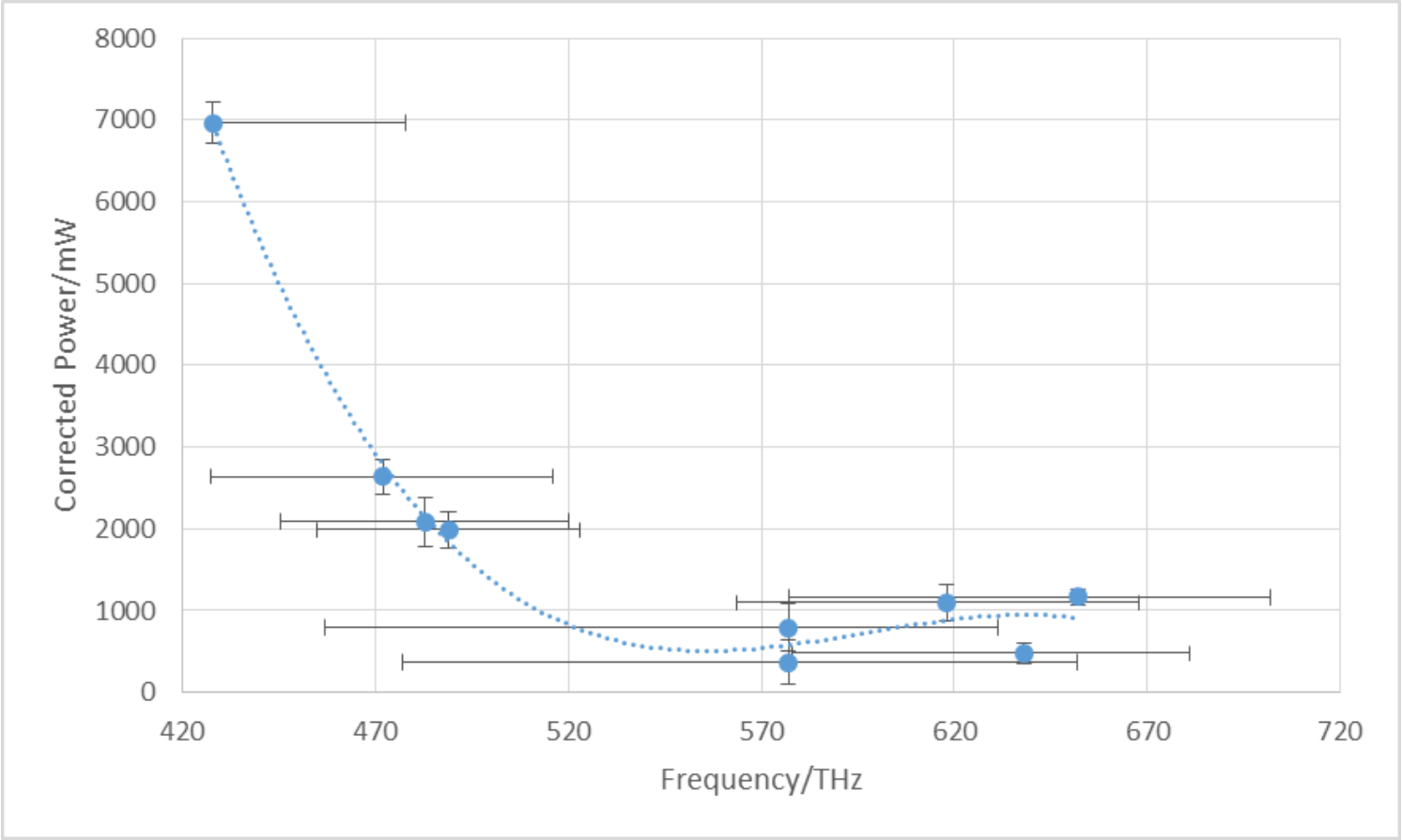

Figure 21: The Variation of Corrected Power Output against Frequency

Due to the enormity of the error bars, there are many interpretations that can be extracted from the graph, therefore no firm conclusion can be obtained.

The following analysis is only appropriate if the dominant wavelength is the reasoning for the power output:

The curve follows a steep negative gradient from 480 to 520 THz which fits the theory of the thermalisation model of a solar cell seen in figure 3. To prove statistically that there is a

negative correlation between frequency and power, a monotonic Spearman Rank correlation test was conducted, see appendix 5. Since the spearman rho value (0.733) is greater than the one-tail critical value for p>0.05 (Spearman, n.d.) (0.714), with a degree of freedom of 7, we can accept that there is statistical significance in the negative direction.

The approximate gradient between 481THz and 507 THz is -0.0017, therefore a decrease of 0.1 mW/% per 5.9 THz. It is unclear whether the curve follows an inverse relationship, with asymptotic behaviour at the local minimum 557 THz or if the curve begins to increase gradually and behave like a cubic graph to form a local maximum at 617 THz.

The initial steep decrease is likely to be due to the thermalisation of the solar panel. The increase in frequency and thus energy of the photons results in excess energy which causes more phonons to be emitted into the lattice of the silicon. This results in thermal vibration causing neighbouring electrons in the semi-conductor to excite, increasing the rest energy of the electron. When these electrons are themselves excited by a photon, the difference in energy levels between its valence band and its conduction band is smaller and thus the power output is smaller. This behaviour is to an extent supported by figure 3, where the maximum spectral intensity is at approximately 500 nm, or 599 THz, which is close to the minimum on the graph at 557 THz.

The negative relationship also supports the Shockley Queisser theory to an extent. In figure 1 the useable electric power decreases linearly from the lowest bandgap of 1.987 eV to the highest 2.621 eV. However, the relationship in this experiment is not linear. The efficiency could level off at higher frequencies due to the balance between higher energy photons released resulting in thermalisation and the tendency for higher wavelengths to recombine without emitting phonons, reducing thermalisation, due to surface recombination, demonstrated in figure 4.

4.2 Graph 2 and Analysis of how tilt angle of the solar panel in relation to the light source affects the power output.

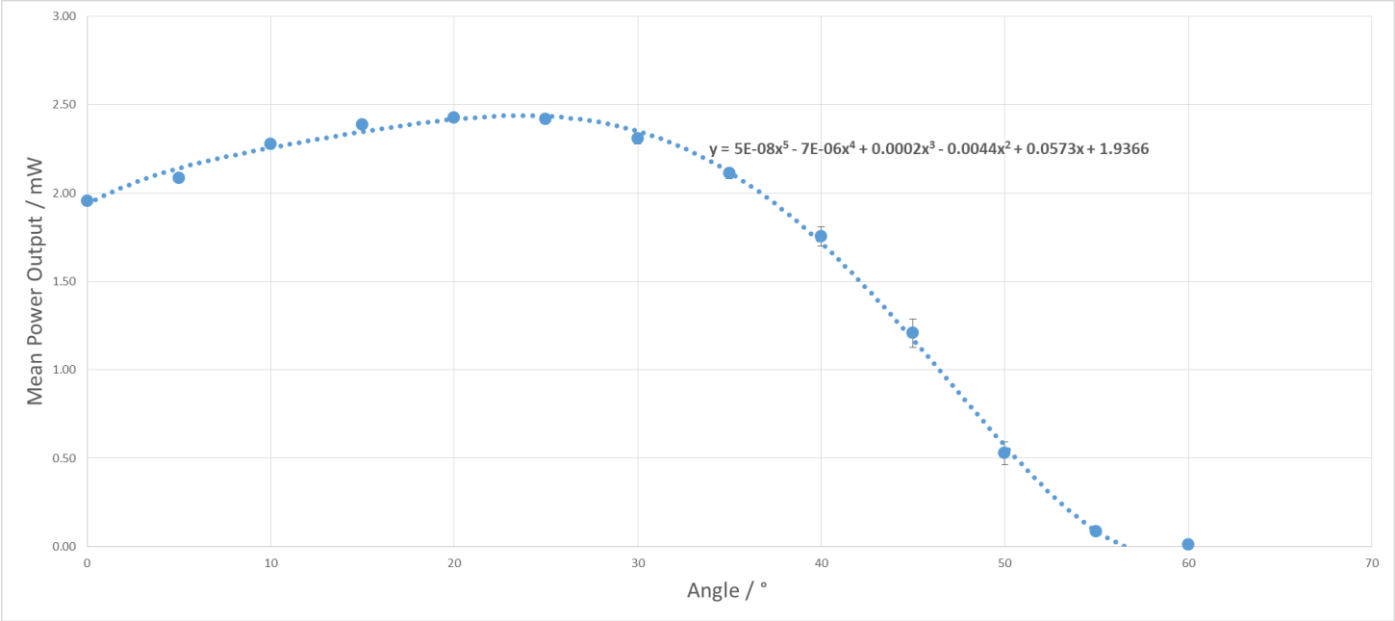

Figure 22: The Variation of Power Output against Inverse Power Squared

The graph shows a gradual incline from 0° to 20° of approximate linear gradient 0.0235, therefore an increase of 0.1 mW per 4.2°. From 40° to 55° the approximate linear gradient is -0.1112, a decrease of 0.1 mW per 0.9°. I differentiated the curve to find the local maximum and therefore optimum angle for efficiency, which is 23.7°. The local minimum was calculated to be at 59°, however as there cannot be negative power, the minimum should be 57° where it intersects the x axis.

The optimum tilt angle is not at 0° but the maximum is shown to be at 23.7°. This is contrary to the model of solar irradiance (figure 5), however supports figure 6, which shows that a slight angle allows for an increase in distance travelled by the photon and thus increases the probability that the photon is absorbed., It demonstrates that this effect increases efficiency to a greater extent than the reduction in solar irradiance caused by the tilt angle.

The rapid decrease from approximately 30° is caused by the tilt angle being greater than the critical angle, resulting in many photons being reflected and not being absorbed, therefore greatly diminishing power output.

When the line intersects the x axis before 90° it suggests that no power can be generated after 57° as the solar cell has reached critical angle, and the light which can still reach the solar panel is reflected and not absorbed. The 60° data point which resulted in 0.01mW instead of 0mW must be due to reflections off the apparatus and back into the solar panel at an angle less than the critical angle. Therefore the steep descent after the maximum is due to the decrease in solar irradiance but also due to total internal reflection where more and more of the light is reflected and not absorbed or refracted through the solar panel medium, until it reaches the critical angle where all light is reflected.

Discussion of the effect of Frequency and Tilt Angle on Power

The results of experiment 1 cannot be validated due to the enormity of the error bars. However, an interpretation from the trendline shows that as frequency and thus energy increases, the power output decreases inversely. The optimum frequency for maximum power output in the visible light spectrum is 480 THz or 624 nm which is a ‘primary red’ colour. However it is unclear as to whether, after the local minimum at 557 THz, there is an increase in power output or it simply levels off. The root cause is undetermined as theoretically an increase in excess energy should lead to an increase in temperature and therefore a decrease in power output. As frequencies after 563 THz has a band gap of 2.22 eV and above, which is double the energy of this PV cell (1.11eV), perhaps some of the photons which have equal or greater than double the band gap are able to excite a neighbouring electron and result in singlet fission. This might explain why there is a gradual

increase after the minimum at 557 THz. However there are many other factors that could have caused this which would need to be investigated in a further study.

The optimum tilt angle is not perpendicular to the light source but at an angle of 23.7°. Despite a decrease in solar irradiance caused by the tilt, light will travel through the silicon for a greater distance and is therefore more likely to be absorbed, increasing power output. After 23.7°, the incident light reaches a critical angle and some light begins to reflect off the surface of the cell and is not absorbed, causing a rapid decrease in efficiency.

This investigation highlights how much temperature reduces efficiency of a PV cell, to the extent where too many photons result in a lower power output. The implications of this study underline the importance of cooling mechanisms for solar cells. Greater wavelength dominated environments such as colours of red could result in greater efficiency for solar panels, whilst areas with blue dominated colours, perhaps reflected from the sea, would be less efficient.

Evaluation

Although both investigations led to several interesting observations, the research question cannot be conclusive. A strength of the study is the ease of repeatability, therefore many trials can be completed improving reliability and removing anomalies. The uncertainties of power were small due to the precision of the multi-meter. However the accuracy could be flawed for particular data points. For example, at 623 THz and 625 THz the power output is not very close to each other despite sharing very similar frequencies. This demonstrates the uncertainty caused by the huge range of frequency values that pass the filter.

The filters allowed ranges of frequencies through which compromised the validity of the findings. Despite knowing the maximum wavelength that the filter let through, other

wavelengths in the range could have influenced the power output and therefore the error bars were large.

In a further investigation, I would change the apparatus to limit the range by choosing smaller range filters or ideally obtain a monochromatic light source, which would single out one specific wavelength. A further limitation was heat from the light source which acted as an uncontrolled variable as it was difficult to regulate how long the lamp was turned on for and therefore how quickly it heated up. As a result, immediately after turning the light source on, the power output of the solar panel decreased, making it difficult to measure a stable reading. To increase reliability, more I would use a more efficient bulb and allow the solar panel to cool between readings.

An interesting investigation to follow from this study, is looking at how power output is affected with infrared light and what is the minimum energy of a photon required for excitation. By experimenting with several types of solar panels with different band gaps, I could find the optimum levels of doping required to maximise efficiency in a particular environment.

Bibliography

(2018, July 25). Retrieved from Penn State University Department of Energy and Mineral Engineering: https://www.e-education.psu.edu/eme812/node/534

Bowden, C. H. (n.d.). *Types of Recombination*. Retrieved July 25, 2018, from PV Education: https://www.pveducation.org/pvcdrom/pn-junctions/types-of-recombination

Challenges for Building Integrated Photovoltaics in the Agder Region. (n.d.). Retrieved from Research Gate: https://www.researchgate.net/publication/268487729_Potential_and_Challenges_for_Building_Integrated_Photovoltaics_in_the_Agder_Region?_sg=SQCJmlgqbvTAzWYKPM0iWotvDhbt1UqF7DTdOui7OVb0FJWFTz8THCrHyZL36tPOvQuxbGlPXA

Current Losses Due to Recombination. (n.d.). Retrieved July 28, 2018, from PVEducation: https://www.pveducation.org/pvcdrom/design/current-losses-due-to-recombination

Dominant Wavelength. (n.d.). Retrieved August 01, 2018, from Collins Dictionary: https://www.collinsdictionary.com/dictionary/english/dominant-wavelength

Estimated Standard Error. (2012, October 7). Retrieved July 27, 2018, from JungMinded: http://jungminded.weebly.com/statistics/estimated-standard-error

Homer, M. B.-J. (2014). *Oxford IB Diploma Programme: Physics Course Companion.* Oxford University Press.

Michl, J. (n.d.). *Josef Michl: Singlet Fission for Solar Cells*. Retrieved July 26, 2018, from YouTube: https://www.youtube.com/watch?v=nM9muHe-hvI

Optoelectronics, Singlet Fission. (2015). Retrieved July 25, 2018, from Cambridge University: https://www.oe.phy.cam.ac.uk/research/photovoltaics/ultrasing

PASPORT Educational Spectrophotometer. (n.d.). Retrieved July 30, 2018, from Pasco: https://www.pasco.com/prodCatalog/OS/OS-8450_pasport-educational-spectrophotometer/index.cfm

Radziemska. (2003, January). Retrieved from Science Direct: https://www.sciencedirect.com/science/article/pii/S0960148102000150

S Riekeberg, P. A. (2006, September). *Decoupling thermalisation from solar cells*. Retrieved July 27, 2018, from Research Gate: https://www.researchgate.net/publication/255970213_Decoupling_thermalisation_from_solar_cells?_sg=nULlGlldr2zgMrxA9Vc9Gm7xZ9YEW_32f5VtJ_6JRFPKg7gWUmZ5RX0Rh8k9BX10dXVLriIzaQ

Shockley Queisser . (n.d.). Retrieved from WikiMedia: https://upload.wikimedia.org/wikipedia/commons/9/99/ShockleyQueisserBreakdown2.svg

Spearman. (n.d.). Retrieved October 8, 2018, from University of York: https://www.york.ac.uk/depts/maths/tables/spearman.pdf

Warren Davis, P. P. (n.d.). Retrieved July 24, 2018, from Physlink: http://www.physlink.com/education/askexperts/ae24.cfm

Appendices

Appendix 1

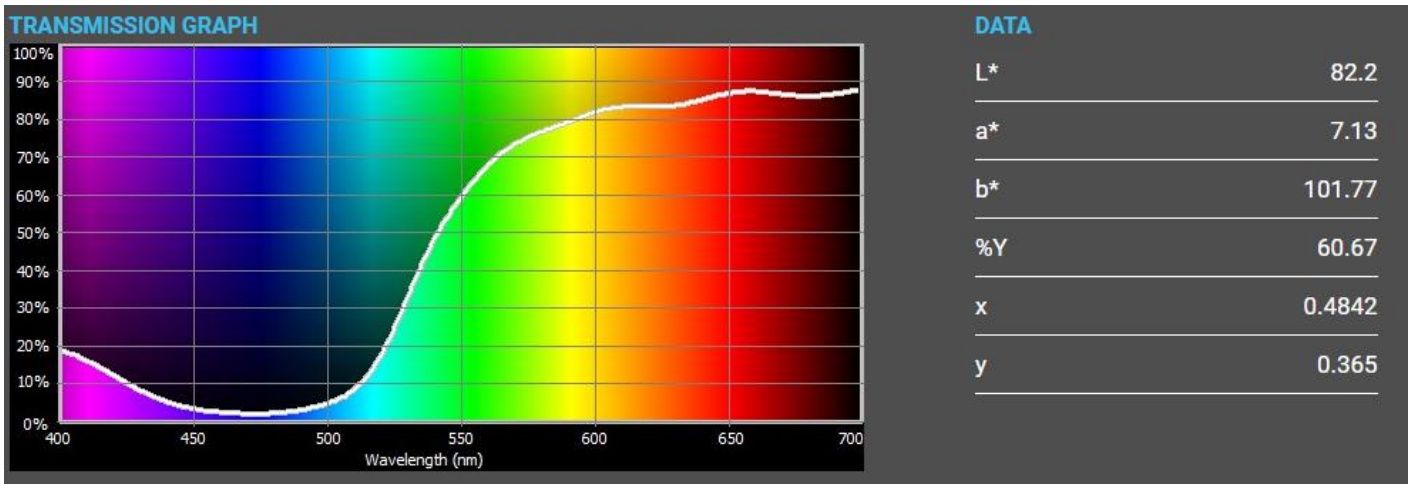

Deep Straw: http://www.cotechfilters.com/filters/015-deep-straw/

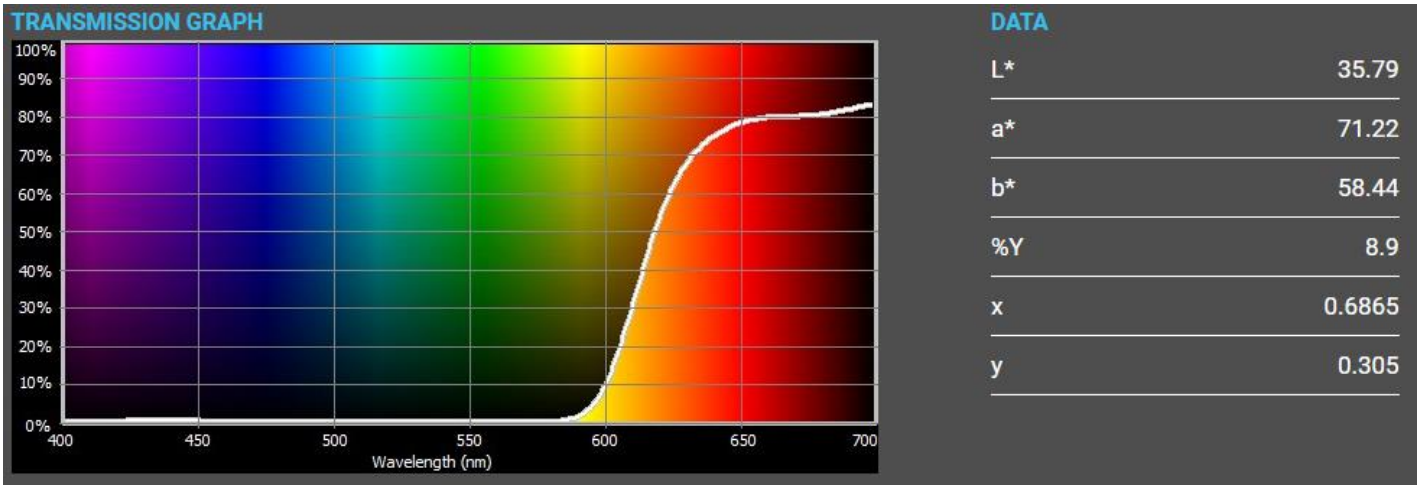

Primary Red: http://www.cotechfilters.com/filters/106-primary-red/

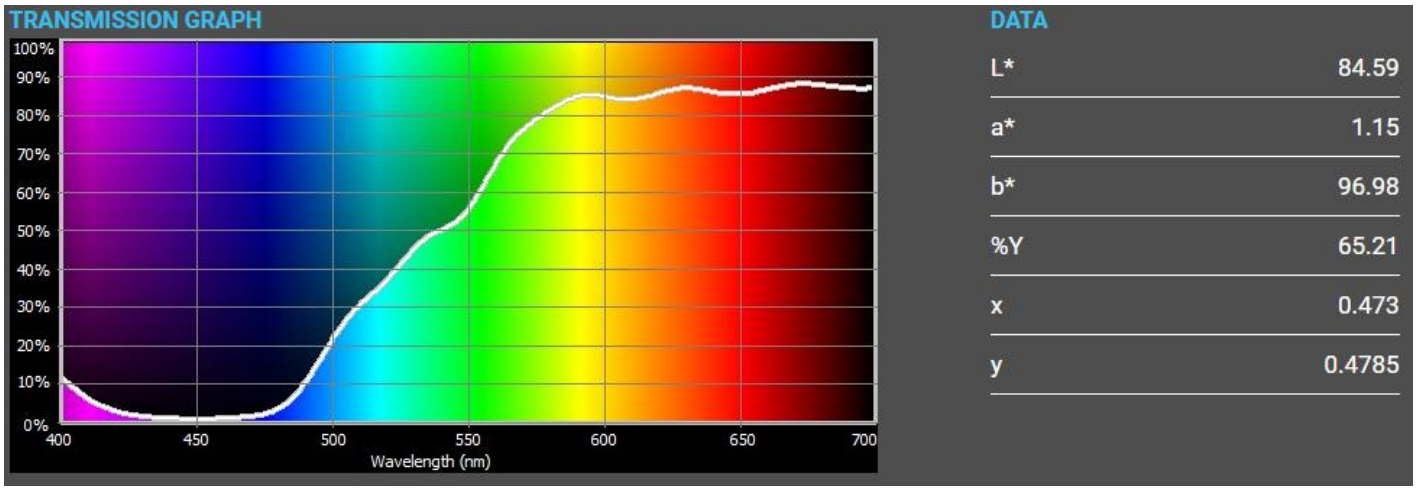

Deep Amber: http://www.cotechfilters.com/filters/104-deep-amber/

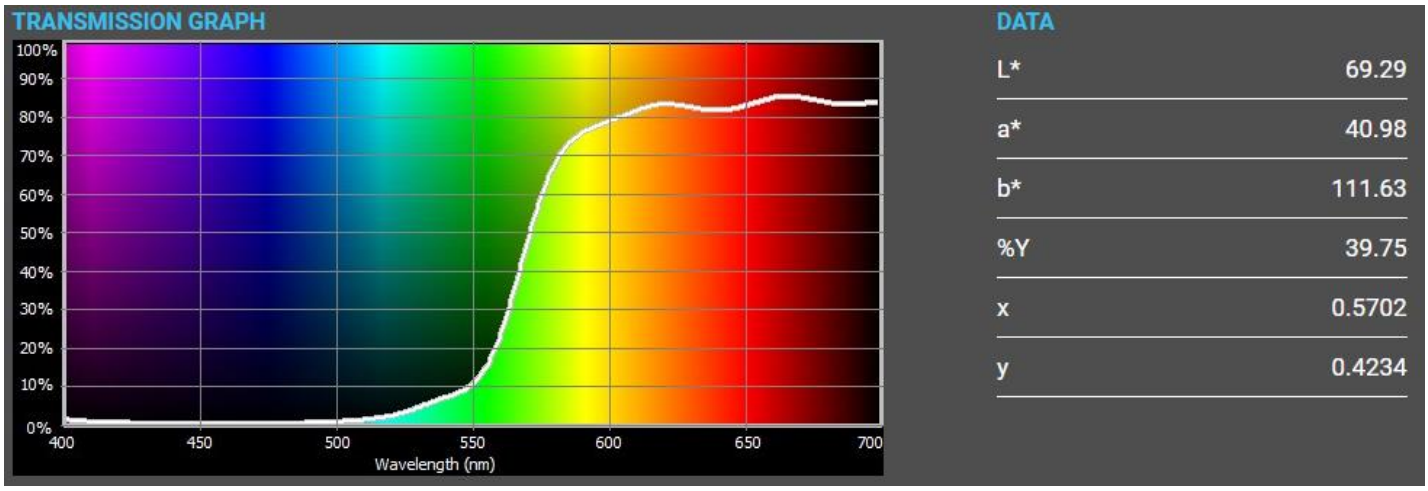

Orange: http://www.cotechfilters.com/filters/105-orange/

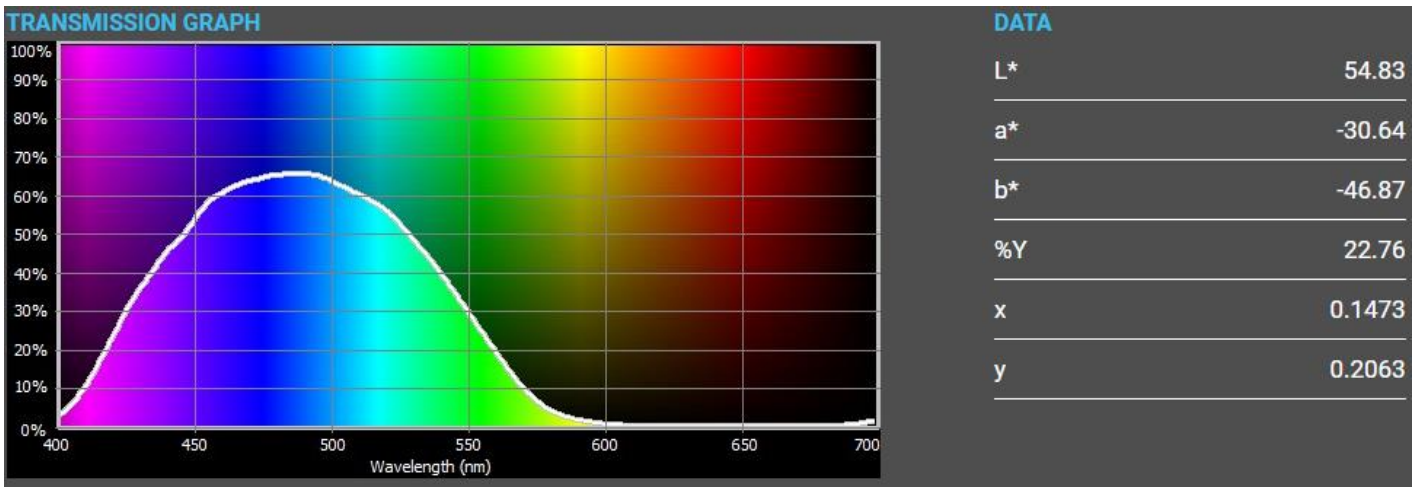

Lagoon Blue: http://www.cotechfilters.com/filters/172-lagoon-blue/

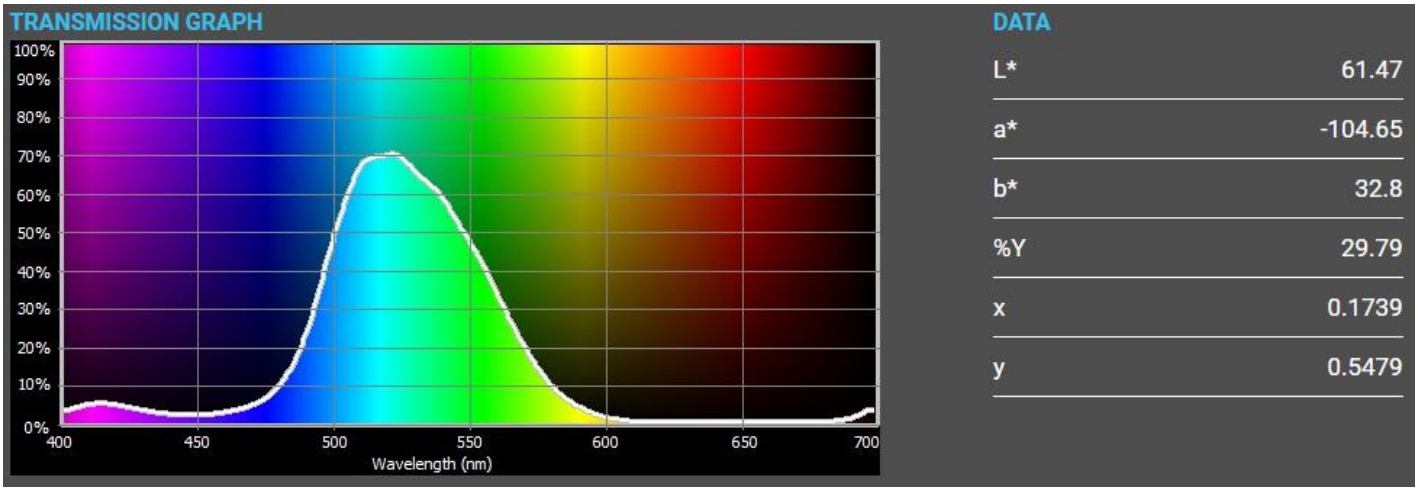

Dark Green: http://www.cotechfilters.com/filters/124-dark-green/

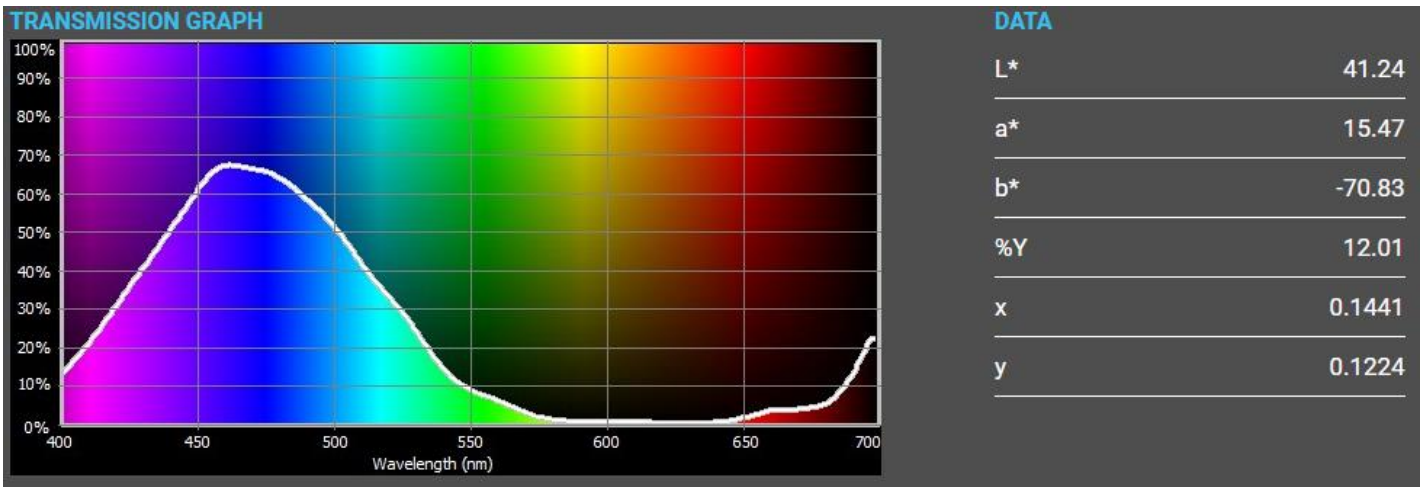

Medium Blue: http://www.cotechfilters.com/filters/132-medium-blue/

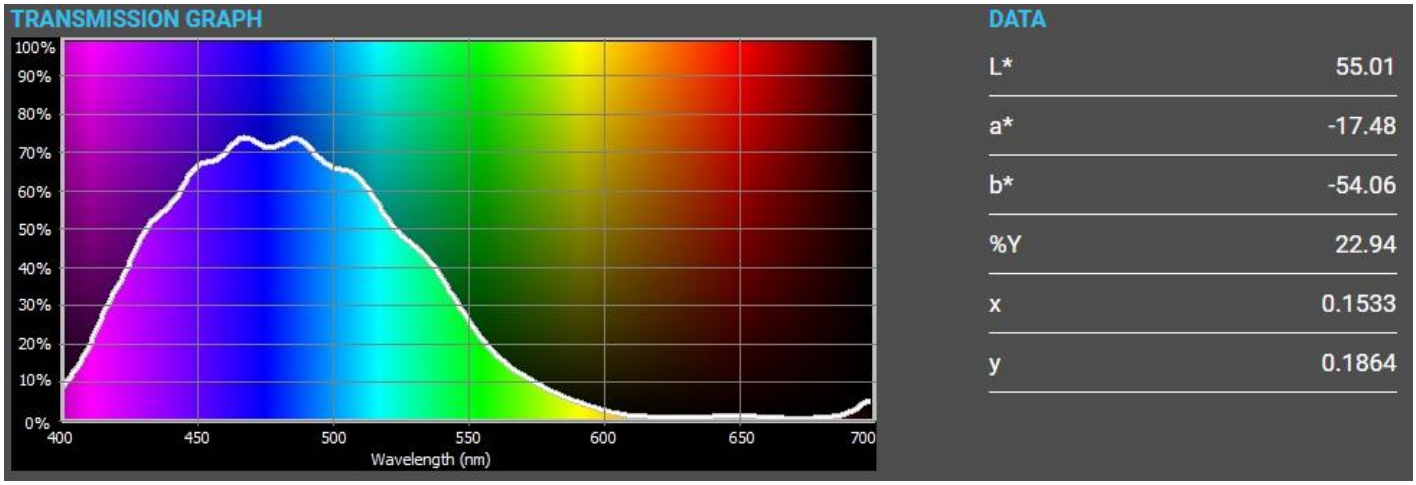

Light Blue: http://www.cotechfilters.com/filters/118-light-blue/

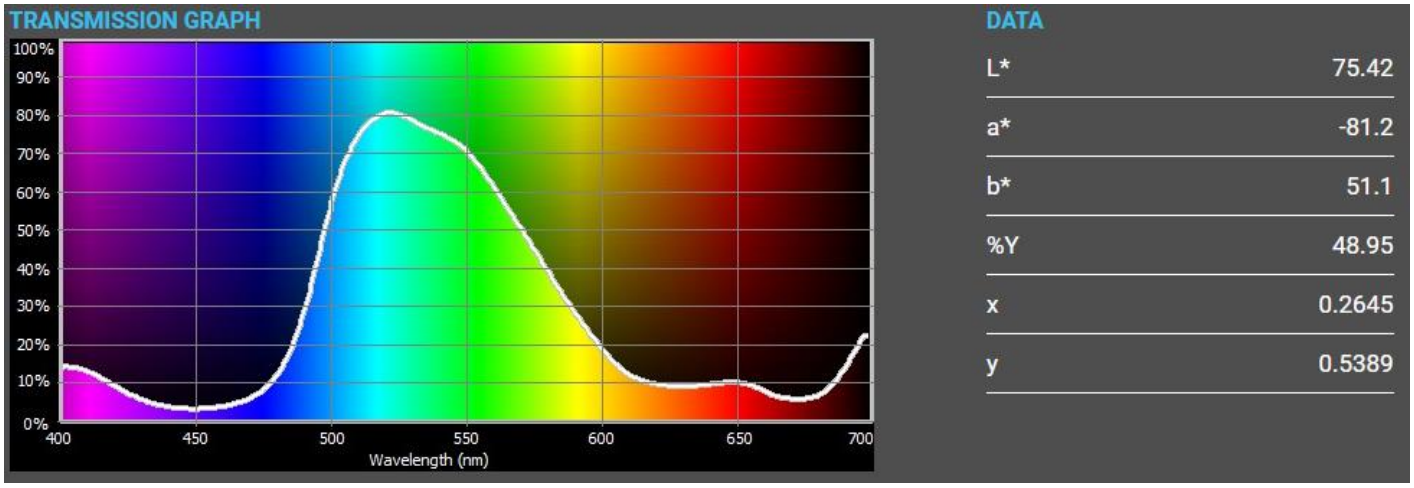

Fern Green: http://www.cotechfilters.com/filters/122-fern-green/

Deep Straw	Trial 1	Trial 2	Trial 3	Trial 4	Trial 5	Mean	Standard Deviation	Standard error
Current/mA	9.30	8.02	8.50	8.56	8.22	8.52	0.49	0.22
Voltage/mV	162.3	141.6	148.8	148.4	143.7	149.0	8.06	3.61
Power/mW	1.51	1.14	1.26	1.27	1.18	1.27	0.13	0.06
Primary Red	Trial 1	Trial 2	Trial 3	Trial 4	Trial 5	Mean	Standard Deviation	Standard error
Current/mA	6.47	5.83	6.02	5.8	5.78	5.98	0.26	0.12
Voltage/mV	112.9	101.5	104.3	101	99.6	103.86	4.77	2.13
Power/mW	0.73	0.59	0.63	0.59	0.58	0.62	0.06	0.03
Deep Amber	Trial 1	Trial 2	Trial 3	Trial 4	Trial 5	Mean	Standard Deviation	Standard error
Current/mA	8.61	8.72	8.70	8.59	8.48	8.62	0.09	0.04
Voltage/mV	152.2	152.2	152.4	149.2	146.4	150.48	2.36	1.06
Power/mW	1.31	1.33	1.33	1.28	1.24	1.30	0.03	0.01
Orange	Trial 1	Trial 2	Trial 3	Trial 4	Trial 5	Mean	Standard Deviation	Standard error
Current/mA	7.86	7.85	7.78	7.72	7.66	7.774	0.08	0.03
Voltage/mV	136.5	136.3	136.3	133.4	133	135.1	1.56	0.70
Power/mW	1.07	1.07	1.06	1.03	1.02	1.05	0.02	0.01
Lagoon Blue	Trial 1	Trial 2	Trial 3	Trial 4	Trial 5	Mean	Standard Deviation	Standard error
Current/mA	4.91	3.61	3.62	3.36	3.46	3.792	0.57	0.25
Voltage/mV	89.6	62.3	62.3	58.4	60.7	66.66	11.56	5.17
Power/mW	0.44	0.22	0.23	0.20	0.21	0.25	0.09	0.04
Dark Green	Trial 1	Trial 2	Trial 3	Trial 4	Trial 5	Mean	Standard Deviation	Standard error
Current/mA	2.3	2.46	2.43	2.43	2.46	2.416	0.06	0.03
Voltage/mV	44.5	47.6	42.5	42.1	42.7	43.88	2.03	0.91
Power/mW	0.10	0.12	0.10	0.10	0.11	0.11	0.01	0.00
Medium Blue	Trial 1	Trial 2	Trial 3	Trial 4	Trial 5	Mean	Standard Deviation	Standard error
Current/mA	2.82	2.88	2.79	2.82	2.95	2.852	0.06	0.03
Voltage/mV	48.3	50.4	48.7	48.3	51.2	49.38	1.20	0.53
Power/mW	0.14	0.15	0.14	0.14	0.15	0.14	0.01	0.00
Light Blue	Trial 1	Trial 2	Trial 3	Trial 4	Trial 5	Mean	Standard Deviation	Standard error
Current/mA	2.47	2.51	2.49	2.41	2.5	2.476	0.04	0.02
Voltage/mV	42.1	43.8	43.2	41.4	43.4	42.78	0.89	0.40
Power/mW	0.10	0.11	0.11	0.10	0.11	0.11	0.00	0.00
Fern Green	Trial 1	Trial 2	Trial 3	Trial 4	Trial 5	Mean	Standard Deviation	Standard error
Current/mA	4.85	4.64	4.73	4.68	4.67	4.714	0.07	0.03
Voltage/mV	83.3	81.4	82.9	80.6	81.4	81.92	1.01	0.45
Power/mW	0.40	0.38	0.39	0.38	0.38	0.39	0.01	0.00

Appendix 2

Distance/cm (±0.05)		10	20	30	40	50	60	70	80	90
	Current/mA (±0.005)	0.31	0.16	0.09	0.06	0.04	0.03	0.02	0.02	0.01
	Voltage/mV (±0.05)	36.6	19.2	10.5	6.7	4.3	3.1	2.4	2	1.5
Trial 1	Power/mW	11.5	3.09	0.945	0.382	0.159	0.0806	0.0480	0.0320	0.0195
	Current/mA (±0.005)	0.32	0.17	0.09	0.06	0.04	0.07	0.02	0.02	0.01
	Voltage/mV (±0.05)	37.7	20	10.3	6.9	4.6	3.4	2.5	2	1.6
Trial 2	Power/mW	12.0	3.42	0.968	0.400	0.179	0.248	0.0525	0.0320	0.0208
	Current/mA (±0.005)	0.32	0.17	0.10	0.06	0.04	0.03	0.02	0.02	0.01
	Voltage/mV (±0.05)	37.4	19.7	11.1	6.9	4.6	3.4	2.5	2	1.6
Trial 3	Power/mW	11.9	3.3293	1.0545	0.4071	0.1794	0.0952	0.0525	0.032	0.0208
	Current/mA (±0.005)	0.32	0.17	0.09	0.06	0.04	0.04	0.02	0.02	0.01
	Voltage/mV (±0.05)	37.2	19.6	10.6	6.8	4.5	3.3	2.5	2.0	1.6
	Power/mW	11.8	3.3	1.0	0.4	0.2	0.1	0.1	0.0	0.0
Mean	$1/\text{Power}^2$	0.0100	0.0025	0.0011	0.0006	0.0004	0.0003	0.0002	0.0002	0.0001

Appendix 3

Percentage Uncertainty			Absolute Uncertainty	
Current	Voltage	Power	Power	$1/\text{Power}^2$
0.1	0.16	0.3	1.31	0.0006
0.3	0.08	0.3	1.11	0.0004
0.5	0.05	0.5	0.51	0.0004
0.7	0.03	0.8	0.30	0.0004
1.1	0.02	1.1	0.19	0.0001
1.5	0.02	1.5	0.21	0.0001
2.0	0.01	2.0	0.10	0.0001
2.5	0.01	2.5	0.08	0.0001
3.2	0.01	3.2	0.07	0.0000

Appendix 4

	Angle/°	0	5	10	15	20	25	30	35	40	45	50	55	60
	Current/mA (±0.005)	10.53	10.93	11.54	11.7	11.71	11.59	11.29	11.02	10.08	8.21	5.04	2.14	0.60
	Voltage/mV (±0.5)	187	191	203	203	203	202	196	191	175	142	89	36	10
Trial 1	Power/mW (±0.005)	1.97	2.09	2.34	2.38	2.38	2.34	2.21	2.10	1.76	1.17	0.45	0.08	0.01
	Current/mA (±0.005)	10.43	10.92	11.42	11.52	11.68	11.85	11.48	10.74	9.59	7.83	5.34	2.12	0.95
	Voltage/mV (±0.5)	181	188	198	200	204	206	200	188	167	136	93	37	16
Trial 2	Power/mW (±0.005)	1.89	2.05	2.26	2.30	2.38	2.44	2.30	2.02	1.60	1.06	0.50	0.08	0.02
	Current/mA (±0.005)	10.6	10.92	11.32	11.78	11.82	11.83	11.7	11.13	10.17	8.52	5.67	1.95	0.84
	Voltage/mV (±0.5)	188	190	196	205	206	206	202	193	176	147	98	33	14
Trial 3	Power/mW (±0.005)	1.99	2.07	2.22	2.41	2.43	2.44	2.36	2.15	1.79	1.25	0.56	0.06	0.01
	Current/mA (±0.005)	10.63	11.23	11.54	11.86	11.92	11.87	11.56	11.24	10.34	8.62	5.7	2.3	0.72
	Voltage/mV (±0.5)	184	192	200	205	206	205	201	194	176	148	98	39	12
Trial 4	Power/mW (±0.005)	1.96	2.16	2.31	2.43	2.46	2.39	2.24	1.98	1.53	0.84	0.22	0.03	0.01
	Current/mA (±0.005)	10.69	10.88	11.36	11.79	11.93	11.82	11.61	11.01	10.15	8.64	5.83	2.71	0.76
	Voltage/mV (±0.5)	185	189	198	204	208	206	202	192	177	149	101	47	12
Trial 5	Power/mW (±0.005)	1.98	2.06	2.25	2.41	2.48	2.43	2.35	2.11	1.80	1.29	0.59	0.13	0.01
	Current/mA (±0.005)	10.58	10.98	11.44	11.73	11.81	11.79	11.53	11.03	10.07	8.36	5.52	2.24	0.77
	Voltage/mV (±0.5)	185.00	190.00	199.00	203.40	205.40	205.00	200.20	191.60	174.20	144.40	95.80	38.40	12.80
Mean	Power/mW (±0.005)	1.96	2.09	2.28	2.39	2.43	2.42	2.31	2.11	1.75	1.21	0.53	0.09	0.01

Appendix 5

Dominant Wavelength/nm (±0.5nm)	Mean Power/Percent Transmission (mW/%)	Wavelength Rank	Power Rank	d	d^2
624	0.06978458	1	1	0	0
598	0.02091873	2	3	-1	1
591	0.02642182	3	2	1	1
578	0.01989170	4	4	0	0
538	0.00788909	5	7	-2	4
515	0.00355871	6	9	-3	9
481	0.01110609	7	6	1	1
479	0.00461741	8	8	0	0
473	0.01172621	9	5	4	16
Sum of d^2	32				
Numerator	192				
n	9				
n^3	729				
Denominator	720				
r	0.733				
df	7				
Critical Value	0.714				
spearman rank correlation coefficient monotonic	0.05				

Appendix 6

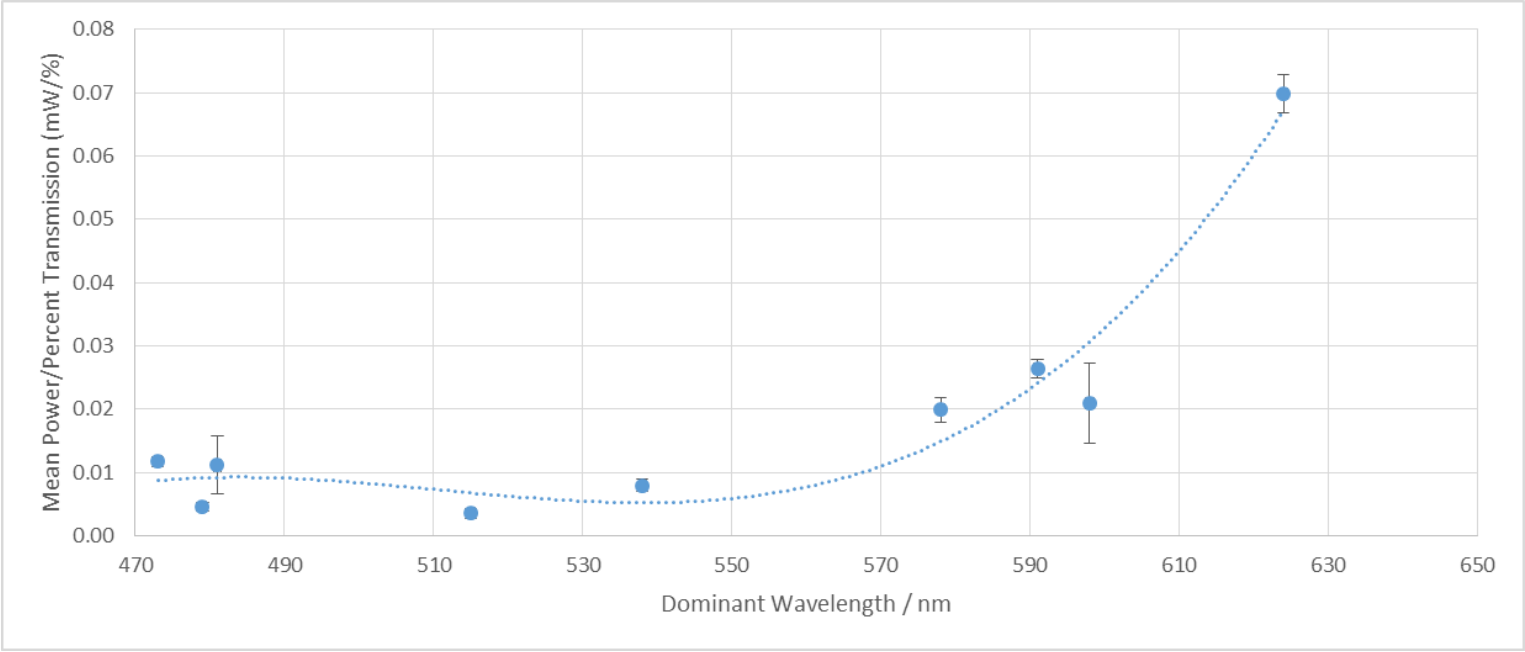

Appendix 7

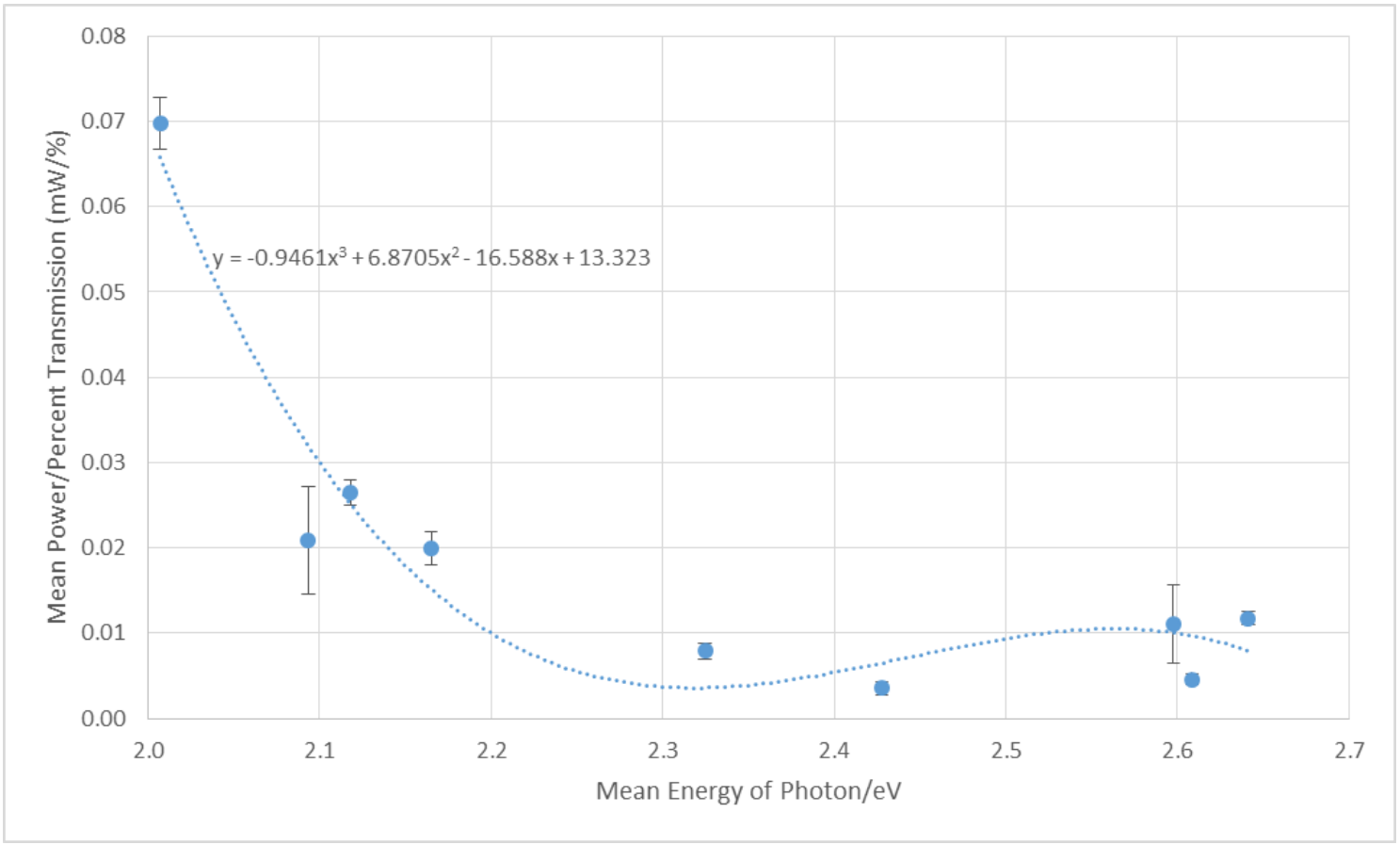

Appendix 8

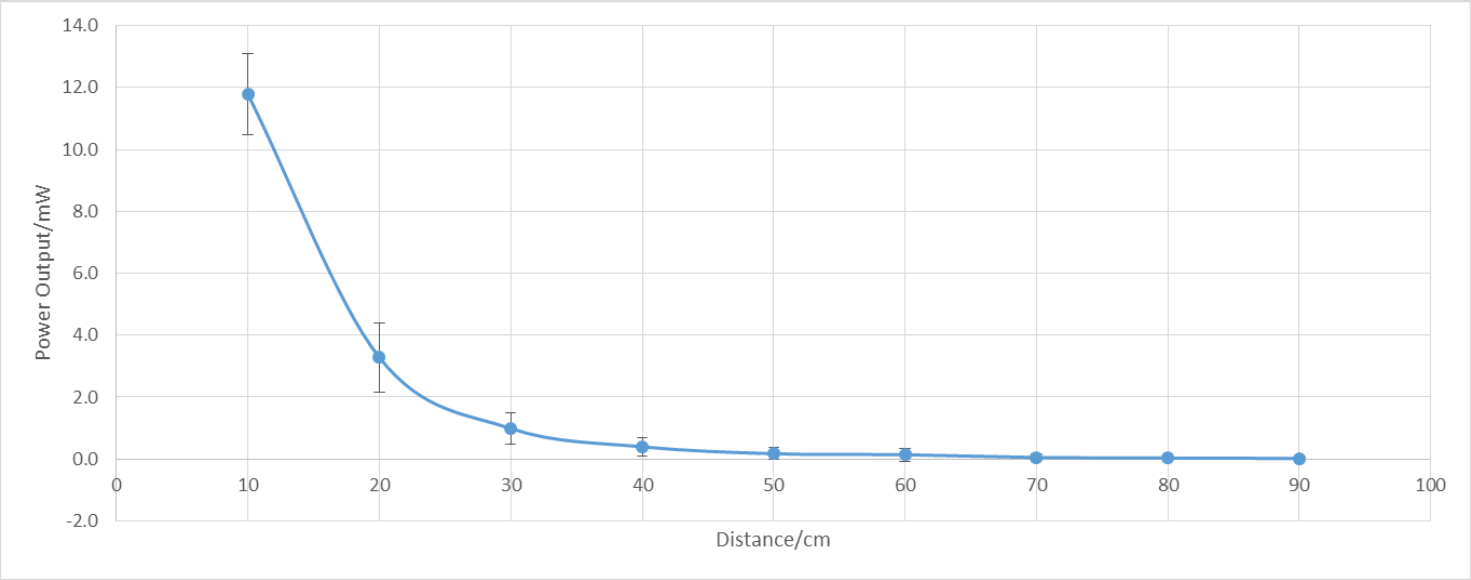
14.0
12.0
10.0
8.0
6.0
4.0
2.0
0.0
-2.0
Power Output/mW
0
10
20
30
40
50
60
70
80
90
100
Distance/cm